

Fragmentation of Nuclei at Intermediate and High Energies in Modified Cascade Model

G. Musulmanbekov, A. Al-Haidary

Abstract

In the frame of intranuclear cascade model additionally to evaporation and fission channels of disintegration of excited remnants in nucleus–nucleus collisions the process of multifragmentation is implemented into the code on the basis of percolation theory. Colliding nuclei are treated as face centered cubic lattices with nucleons occupying the nodes of the lattice. The site – bond percolation model is used. The code can be applied for calculation of fragmentation of nuclei in spallation and multifragmentation reactions.

1 Introduction

Intranuclear cascade model is one of the basic tools for analyzing spallation and multifragmentation processes in nuclear collisions. In traditional cascade model of hadron - nucleus and nucleus - nucleus interactions particle production is treated in two stages. In the first, fast, stage intranuclear cascade is developed inside target and (or) projectile nuclei and some nucleons from target and projectile nuclei accompanied with mesons are knocked out of them. On the second stage residual nuclei, in general excited, can be divided into two remnants according to fission channel or evaporate protons, neutrons and light nuclei including helium isotopes. However, according to experimental data at intermediate energies the third competing process, multifragmentation, comes into play – excited remnants break up into intermediate mass fragments (IMF). There are two approaches for theoretical description of multifragmentation: dynamical and statistical. In statistical multifragmentation models excited remnant comes to thermal equilibrium

state and then expands reaching the freeze-out volume. At this point it fragments into neutrons, light charged particles and IMFs. In dynamical models IMFs are formed at the fast stage of nuclear collision via dynamical forces between nucleons during the evolution of the total system of interacting projectile and target. In this case the whole system and its parts (projectile and target remnants) never pass through thermal equilibrium states.

There is one more approach for description of the process of multifragmentation: percolation theory. Percolation models treat nucleus as a lattice with nucleons located at nodes of lattice. Moreover, it turned out that results of percolation calculations depend significantly upon the details of the lattice structure. For reasons of computational convenience simple cubic lattice has been most frequently used in multifragmentation simulations[1]. It has been shown in papers[2, 3] that face centered cubic lattice is more appropriate to reproducing the experimental fragments mass distributions and their energy spectra.

Although lattice simulations have been found to reproduce multifragmentation data surprisingly well, there has been a little examination of the role of lattice in arrangement of nucleons inside nuclei. Lattices were more employed as computational techniques, rather than as formal nuclear models. The appearance of solid state models of nuclear structure can be dated from the paper of Pauling in 1965 [4, 5, 6]. The most attractive one among them is face-centered-cubic lattice (FCC) model proposed by Cook and Dallacasa[6] because it brings together shell, liquid-drop and cluster characteristics, given by conventional models, within a single theoretical framework. Unique among other nuclear lattice models FCC reproduces the entire sequence of allowed nucleon states as found in the shell model.

In the present paper we further develop the modified intranuclear cascade-evaporation code, (MCAS) elaborated by one of the authors [7], with the aim of inclusion multifragmentation channels. The word "modified" relates to implementation of "formation time" concept into traditional cascade calculations, as described in Section 3. Goodness of fit of MCAS to experimental data on multiparticle production in nucleus – nucleus collisions at intermediate energies and moderately high energies (up to 10–20 GeV/n) have been tested in papers[7, 8] Since traditional cascade models consider nuclear structure as dilute fermi gas we rebuild it in the frame of lattice nuclear model. For this purpose we implement FCC lattice arrangements of nucleons to building structure of colliding nuclei according to algorithm proposed in paper[9] (Section 2). Calculations of multifragmentation channels are performed on

the basis of bond–site model of percolation theory (Section 4). Comparison with experimental data are given in Section 5.

2 FCC lattice model of nuclear structure

FCC packing of nucleons, occupying lattice sites with alternating layers of protons and neutrons, is seen as consisting of four interpenetrating cubes. A nearest–neighbor distance is chosen to be about 2.0262 fm that produces the known core density of nuclei (0.17 nucleons/fm³). The essence of the geometry of FCC model can be shown using the quantum numbers that are assigned to each nucleon in the conventional shell model[9]. It is known that a nucleon’s distance from the center of the nucleus determines principal quantum number **n**. The distance of nucleon from ”nuclear spin axis” determines its total angular momentum (quantum number **j**). Finally, the distance of each nucleon from $y - z$ plane determines its magnetic quantum number **m**. The inherent simplicity of the FCC model is evident in the FCC definitions of the eigenvalues:

$$\mathbf{n} = (|x| + |y| + |z| - 3)/2, \quad (1)$$

$$\mathbf{j} = (|x| + |y| - 1)/2, \quad (2)$$

$$|\mathbf{m}| = |x|/2, \quad (3)$$

where the sign of the **m** value is determined by the intrinsic spin orientation on the nucleon in the antiferromagnetic lattice (spin up = $\frac{1}{2}$ and spin down = $-\frac{1}{2}$). Conversely, the coordinate values can be determined solely in terms of the eigenvalues:

$$x = |2m|(-1)^{m+\frac{1}{2}}, \quad (4)$$

$$y = (2j + 1 - |x|)(-1)^{i+j+m+\frac{1}{2}}, \quad (5)$$

$$z = (2n + 3 - |x| - |y|)(-1)^{i+n-j-1}, \quad (6)$$

where **i** is isotopic quantum number. Therefore, knowing the full set of eigenvalues for a given set of nucleons, the configuration of those nucleons in 3–D space relative to the nuclear center can be determined unambiguously. Using the fermi coordinates of each nucleon, the mean radius of the nucleus

with A nucleons is defined as

$$R[A] = R_{nucleon} + \frac{1}{A} \sum^A r_j, \quad (7)$$

where r is the Euclidean distance of each nucleon, $\sqrt{x_j^2 + y_j^2 + z_j^2}$, from the origin and $R_{nucleon}$ is the nucleon radius. The calculated charged radii for various nuclei are in a good agreement with experiment.

3 Intranuclear Cascade with Nuclear Lattice Model

Nucleon coordinates (4 – 6) for target (projectile) nucleus are generated in accordance to algorithm given in paper[10]. For each nuclear collision lattices of target and projectile nuclei are oriented randomly in relation to the collision axes. This random orientation of nuclear lattice in 3–D space mimics Woods – Saxon distribution of nuclear density for medium and heavy nuclei. Nucleon momenta inside the nucleus, \mathbf{p} , are generated uniformly in the space $0 \leq |\mathbf{p}| \leq p_F$. The bound Fermi momentum p_F relates to the local nucleon density as

$$p_F = (3\pi^2)^{1/3} h \rho^{1/3}(r). \quad (8)$$

Inelastic collision of two nuclei is a incoherent superposition of baryon - baryon, meson - baryon and meson - meson elastic and inelastic interactions. Elastic and inelastic cross sections and kinematical features of elastic scattering are taken from experiments. Description of inelastic event generator is given in Appendix. All interactions are arranged into four groups.

Group C - interactions of the nucleons of the projectile nucleus with those from the target nucleus. All secondary particles produced in any group of interactions are considered as cascade particles.

Group A - interactions of the cascade particles with the nucleons of the target nucleus;

Group B - interactions of the cascade particles with the nucleons of the incident nucleus;

Group D - so called "cascade - cascade" interactions — interactions of cascade particles with each other.

The probability of interaction of any particles i and j is defined by black disk approximation:

$$P(b_{ij}^2) = \Theta(b_{ij}^2 - \sigma_{tot}/\pi), \quad (9)$$

where b_{ij} – impact parameter between hadrons i and j , σ_{tot} – their total cross section. Cross sections of resonances in subsequent interactions are taken to be the same as for stable particles. Evolution of the interacting system is considered as follows. At some instant of time t all possible interacting pairs in each group (A,B,C,D) are determined. Among all possible interactions that one is chosen to be the first in order which realizes before others, i.e. $\Delta t = \min\{t_i\}$; then the positions of both nuclei and all cascade particles are moved to new ones corresponding to a new instant of time $t_i \rightarrow t_i + \Delta t$. Since the formation of hadronic states of secondary particles takes for some time we apply for considerations of their subsequent interactions the concept of formation time (zone). The formation time relates to the development of cross section of the produced particle during its propagation inside the nuclear medium. We use the exponential form of evolution of cross sections until the subsequent collision occurs

$$\sigma_2^l = \sigma_1^I (1 - (1 - x^l) e^{-\tau/(\gamma\tau_0)}) \quad (10)$$

for leading particle,

$$\sigma_2^m = \sigma_1^m - (\sigma_1^m - x^m \sigma_1^I) e^{-\tau_1/(\gamma\tau_0)} \quad (11)$$

for m - th produced particle, where σ_1^I - normal cross section of the incident particle in the first collision, σ_2^l - cross section of the remnant of the projectile (leading particle) in the second collision, σ_2^m - cross section of the m - th produced particle, σ_1^m - cross section for this type of particles in the normal state, γ — Lorentz-factor and τ_0 is adjustable parameter corresponding to the mean value of the formation time in the rest frame of the particle. For $r + 1$ - th inelastic rescattering of the incident particle the cross section is defined as

$$\sigma_{r+1}^l = \sigma_1^I \prod_{i=1}^r (1 - (1 - x_i^l) e^{-\tau_i/(\gamma_i\tau_0)}) \quad (12)$$

Among secondaries s-wave resonances (deltas, rho and omega mesons) can be produced. Hadronic event generator is briefly described in Appendix.

During evolution of the system produced resonances may decay before their subsequent interactions. It is checked both for all interactions and decay of resonances whether the Pauli principle is satisfied. Cascade stage of particle generation is completed when all cascade particles have left both nuclei or partly absorbed by them. So, the first, fast stage of multiparticle production of nuclear collision is over. After replacing fermi – gas nuclear model by FCC lattice we compared the results of simulation of both models on multiparticle production in intermediate and high energy nuclear collisions and found out that they are identical. First measurable characteristic of nucleus – nucleus collision is reaction cross section. In intranuclear cascade models it is defined by the ratio of realized inelastic collisions number, N^{in} , to the total number of trials, N^{trial} :

$$\sigma^{reac} = \frac{N^{in}}{N^{trial}} \pi (R_A + R_B + \Delta)^2, \quad (13)$$

where $R_{A,B}$ – radii of colliding nuclei and Δ – radius of strong interaction. Fermi – gas and FCC lattice models agree with accuracy 5 percent.

4 Fragmentation of Excited Remnants

The number and total charge of remaining nucleons in each remnant specify mass and charge numbers of the residual nuclei. In general, remnants are in excited state and possess angular momentum. Excitation energy of each remnant nucleus is determined by the energy of absorbed particles and "holes" leaving by knocked out nucleons during intranuclear cascade process. Momentum and angular momentum of the residual nucleus is evaluated by momentum conservation law sequentially followed for each intranuclear interaction. Thus, there are three competing processes for disintegration of excited remnant nucleus: evaporation, fission and multifragmentation. In standard intranuclear cascade model only first two processes are taken into account[11]. Our task is to implement multifragmentation on the basis of percolation theory and define the relative weights of above three competing processes. We apply site–bond percolation model. In relation to nucleus we assume that nucleons occupying lattice sites are connected with their neighbors via bonds which schematically represent two body nuclear forces. In the fast stage, during the development of intranuclear cascade some nucleons occupying the sites of FCC lattice of target (projectile) nucleus are knocked

out leaving the "holes" at that sites. We say that these sites are broken. The ratio of the number of broken sites to the total number of sites (mass number of target or projectile) characterizes the destruction degree of the target (projectile) nucleus after cascade stage. This ratio depends on the collision energy, mass numbers of colliding nuclei and, particularly, on impact parameter of collision. In peripheral collisions mainly peripheral nucleons are knocked out, that means that remaining nucleons with high probability form one cluster in which all sites are occupied. In collisions with more centrality that corresponds intermediate and small impact parameters nucleons are knocked out mainly from nucleus interior and target (projectile) remnant represents the lattice with some sites broken. As mentioned above, remnants, in general, are in excited states. The larger impact parameter the less is the number of broken sites and the less is the excitation energy of remnant. This initial condition is preferable for equilibration and thermalization of excited nuclear media that allows one to use evaporation and fission mechanisms of subsequent disintegration of excited remnant. With increasing centrality of collision the number of broken sites increases (large destruction) that leads to increasing excitation energy of remnant nucleus. For this case there is no conventional understanding of mechanism of disintegration of excited remnant (thermal break-up with statistical multifragmentation, liquid-gas phase transition, sequential evaporation, cold break-up like shattering of glass). However, it is obvious that at sizable destruction of the remnant there is no room for equilibration and thermalization over the whole volume of the remnant.

For excited remnant disintegration we specify bond breaking probability, as input parameter p_{bond} , in the form of impact parameter dependence:

$$p_{bond}(b) = p_{bond}(0) \sqrt{1 - \frac{b^2}{(R_A + R_B)^2}}, \quad (14)$$

where R_A and R_B are radii of colliding nuclei. This anzatze can be derived from the considerations of collision geometry. Then cluster counting algorithm, elaborated by authors, looks for clusters (fragments): whether neighbor nucleons are connected via bonds or not. Only first-nearest and second-nearest neighbors are taken into account in counting algorithm. In the initial FCC lattice each nucleon has 12 first-nearest neighbors at distance 2.0262 fm and 6 second-nearest neighbors at 2.8655 fm. As a result of this counting algorithm we have mass and charge distribution of fragments.

Although this approach is statistical and the probability of any bond to be broken does not depend on its position, the probability of disintegration of remnant on multiple clusters (fragments) will be higher in the vicinity of regions with broken sites concentration. From this it follows that the process of multifragmentation is influenced by dynamics of collision, i.e. according to our scenario it is not pure statistical process.

Now we should specify energetic characteristics of radiated fragments. In general, in its proper frame the remnant possesses rotational energy, E^{rot} , and excitation energy, E^* , which are converted into the summary of rotational, E_{fr}^{rot} , and kinetic energies of fragments, E_{fr}^{kin} , their excitation energies, E_{fr}^* , and the energy of coulomb interactions of fragments, E_{fr}^{coul} :

$$E^{rot} + E^* = E_{fr}^{rot} + E_{fr}^{kin} + E_{fr}^* + E_{fr}^{coul} = \sum E_i^{rot} + \sum E^{kin}(A_i, Z_i) + \sum E^*(A_i, Z_i) + \frac{1}{2} \sum \frac{Z_i Z_j}{r_{ij}}. \quad (15)$$

In standard intranuclear cascade model the contribution of rotational energy, E_{fr}^{rot} , is small compared with other terms, at least for light nuclei, as projectiles. Whether it is the case in reality or not is unknown. Large rotational energies could be realized in this approach if we include nuclear viscosity. In current calculations we neglect the first term. Moreover, for computational convenience we make additional simplifications in Eq. (15). As coulomb repulsion of charged fragments raises their kinetic energies we define resulting kinetic energies of fragments as follows:

$$E_{fr}^{kin} + E_{fr}^{coul} = \sum E^{kin}(A_i, Z_i) + \frac{1}{2} \sum \frac{Z_i Z_j}{r_{ij}} = \sum \varepsilon_i(A_i, Z_i). \quad (16)$$

Another simplification concerns with excitation of fragments: we assume that the only one fragment among others is excited, that one mass number of which is maximal. It is justified, particularly, when comparing model with data obtained at inverse kinematics because experimental setup registers majority of radioactive fragments as well. Therefore, the excitation energy of remnant, E^* , is converted into kinetic energies of fragments and excitation energy of the fragment with maximal mass:

$$E^* = \sum \varepsilon_i(A_i, Z_i) + E^*(A_{\max}, Z_{\max}) \quad (17)$$

With this simplifications we generate energy distribution of fragments applying considerations proposed in paper[12]. Before the collision the nucleons have a momentum distribution that is uniform inside the Fermi sphere

of radius p_F . After the collision the distribution in vicinity of the beam propagation is wider because of intranuclear interactions accompanied by local excitation of nuclear medium. It can be chosen in the form

$$n(\varepsilon) \propto 1 / \left\{ 1 + \exp \left[\frac{\varepsilon - \varepsilon_F}{T_{eff}} \right] \right\}, \quad (18)$$

where $\varepsilon = p^2/2m$, ε_F is boundary Fermi energy. The "effective temperature" is given by

$$T_{eff} = cE^*/N_{br}, \quad (19)$$

where c is adjustable parameter and N_{br} is the number of broken sites. Kinetic energies of nucleons composing the fragment are generated according to distribution (18), and summing up all vector momenta directed randomly in 3D space we obtain the momentum of the fragment. In such a way we generate momenta of all produced fragments. The remaining part of the remnant excitation energy, (17), is assigned to the fragment with maximal mass number. And, of course, we take into account energy – momentum conservation law for the whole reaction.

5 Comparison with Experiment

Observation of residues emerging from spallation reactions in direct kinematic still remains a difficult task. Collisions of proton and light nuclei with heavy ions performed at GSI in inverse kinematics allows one to determine the production of residues prior to β decay. It gives a good opportunity of intercomparison of available data with models for understanding the mechanism of reactions which is far from satisfactory. Until now the calculations are performed by different versions of intranuclear cascade followed by evaporation model. As seen from the previous section, our model additionally includes multifragmentation channels in frame of percolation approach. Now we should define the values of input parameters, which are bond breaking probability, $p_{bond}(0)$, in Eq. (14) and constant c in Eq. (19). $p_{bond}(0)$ depends on energy of collision and type of reaction. For specific reaction, it is obvious that site and bond breaking probabilities are small at low energies and start growing with energy reaching the constant values at the regime called "limiting fragmentation". Limiting fragmentation is reached at different energies for different reactions. Therefore, at low energies the dominating

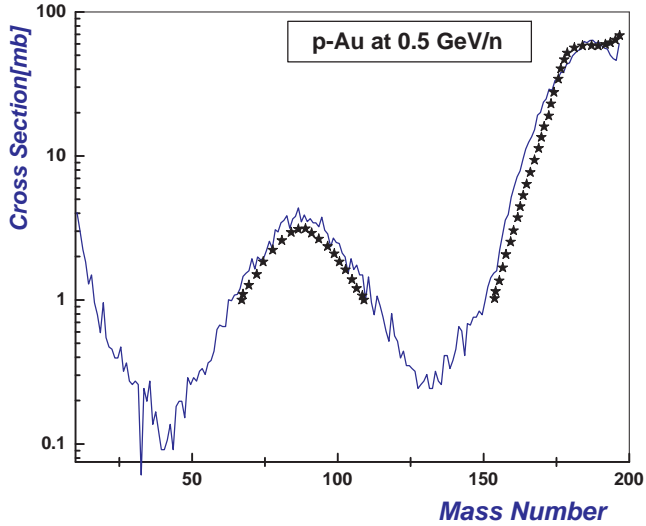


Figure 1: Mass distribution of residues produced in 0.5 GeV proton induced reaction on ^{197}Au . Data are from paper[13].

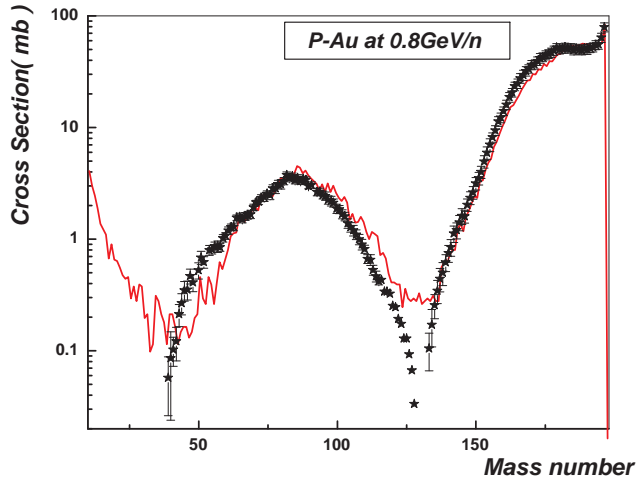


Figure 2: Mass distribution of residues in the reaction $^{197}\text{Au} + \text{p}$ at 800 A MeV. Data are taken from paper[14].

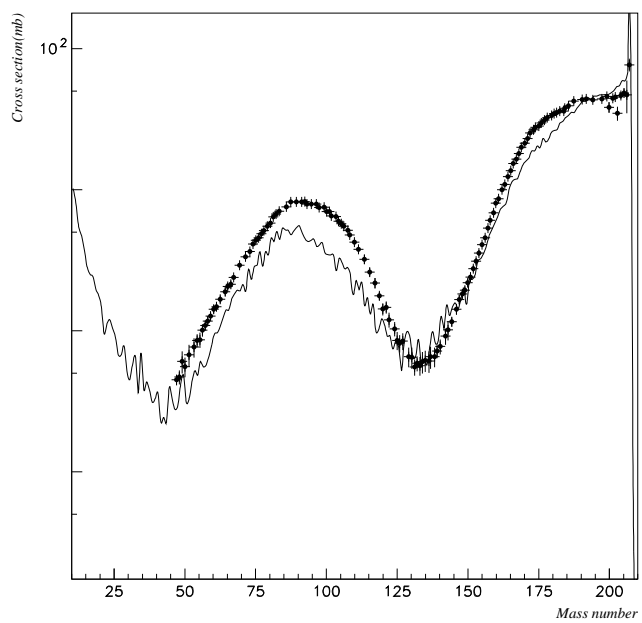


Figure 3: Mass distribution of residues in the reaction $^{208}\text{Pb} + \text{p}$ at 1 A GeV. Data are taken from paper[15].

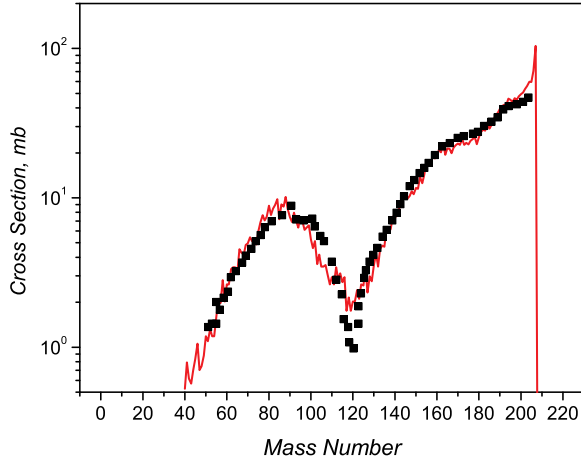


Figure 4: Mass distribution of residues in the reaction $^{208}\text{Pb} + \text{d}$ at 1 A GeV. Data are taken from paper[16].

mechanisms of disintegration of excited remnant are evaporation and fission. While energy of collision grows the contribution of multifragmentation processes starts increasing depending on site and bond breaking probabilities. Since number of broken sites is defined automatically during the development of intranuclear cascade, only bond breaking probability remains to be input parameter. For proton induced reactions $p_{bond}(0)$ changes from 0, at incident proton energy of few tens of MeV, to 0.77 at limiting fragmentation energy (3 – 4 GeV). What concerns with parameter c in Eq. (19), it's value is chosen to be 0.7, energy independent, for all types of reactions. Comparison of the model calculations for mass distributions in spallation reactions pAu, at 0.5 and 0.8 GeV and pPb at 1 GeV and dPb at 2 GeV are shown on Figs. 1 – 4. As seen from figures, at energies lower than those corresponding limiting fragmentation regime mass yield distributions of residues in proton induced reactions have well pronounced bell – shaped central part which emerges from the contribution of fission channels. Evaporation channels give dominating contribution to the right peak of the distribution with plateau at high masses of residues. The values of level density parameters for evaporation and fission are taken to be $0.1A \text{ MeV}^{-1}$, the same for both and independent on type of

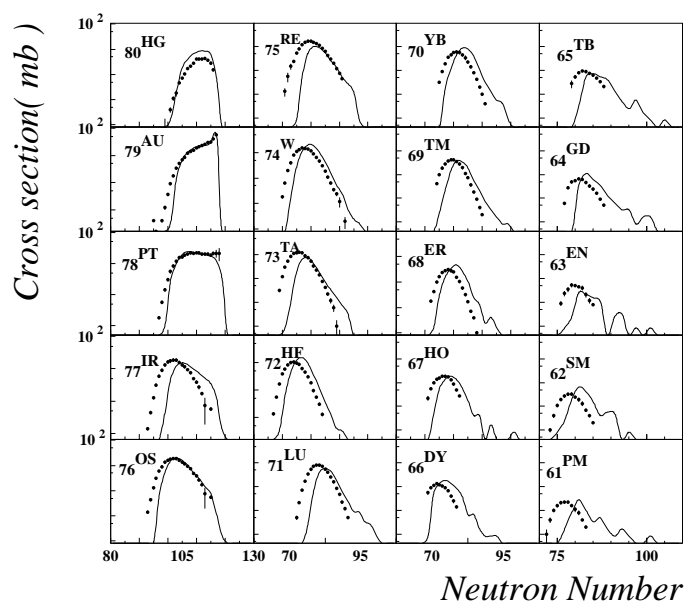


Figure 5: Isotopic distribution of spallation residues in reaction 0.8 GeV ^{197}Au on proton. Data are taken from the paper[14].

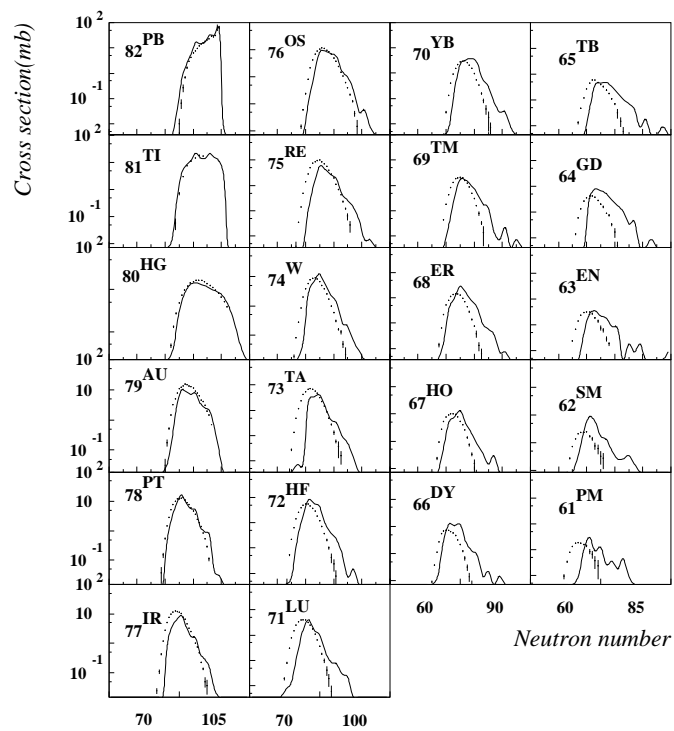


Figure 6: Isotopic distribution of spallation residues in reaction 1 GeV ^{208}Pb on proton[15].

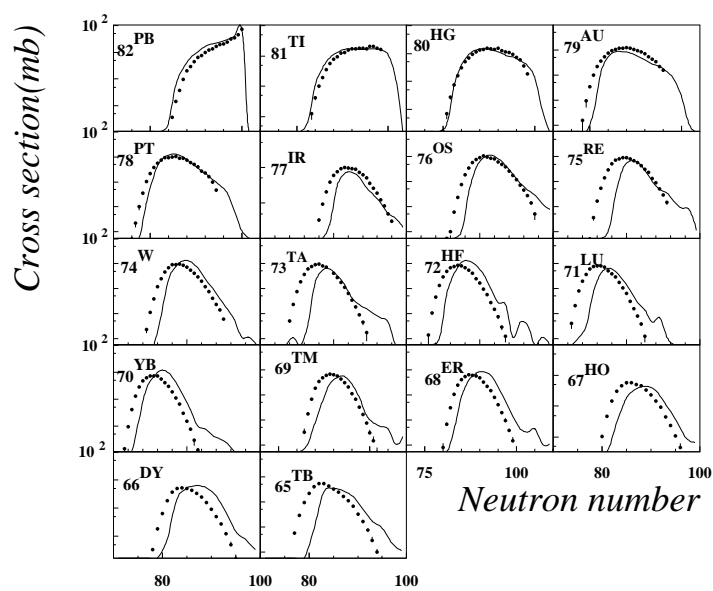


Figure 7: Isotopic distribution of spallation residues in reaction 1 GeV ^{208}Pb on deuterium. Data are from the paper[16].

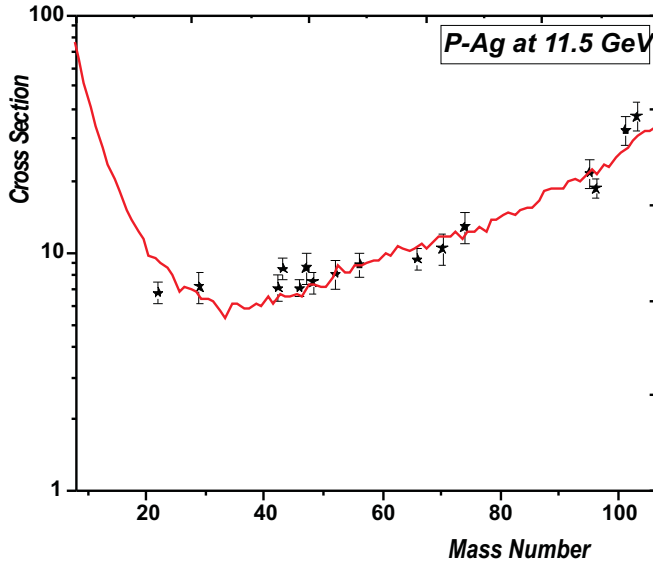


Figure 8: Mass distribution of fragments in the reaction $p + {}^{108}\text{Ag}$ at 11.5 GeV. Data are taken from paper [17].

reaction and collision energy. Figures 5– 7 show the isotopic distributions of residues produced in the following reactions: $p\text{Au}$ at 0.8 GeV, $p\text{Pb}$ at 1 GeV and deuteron – Pb at 2 GeV. Calculated distributions are shifted to neutron – rich isotopes yield for lighter residues. We hope that underestimation of proton–rich isotopes and overestimation of neutron–rich isotopes could be corrected by better description of proton – neutron competition in fission – evaporation channels. As bombarding energy increases, so does the contribution of multifragmentation channels and, correspondingly, contribution of evaporation and fission channels decreases. It leads to filling of dips at both sides of central bell – shaped part and decreasing of the height of right peak. As mentioned above, rising collision energy leads to increasing number of broken sites and bonds in nuclear lattices. This, in turn, results in increasing multifragmentation channels yield. Mass distributions of fragments in for proton and carbon induced reaction on Ag and Au at energies corresponding limiting fragmentation regime are given in Figures 8 – 10.

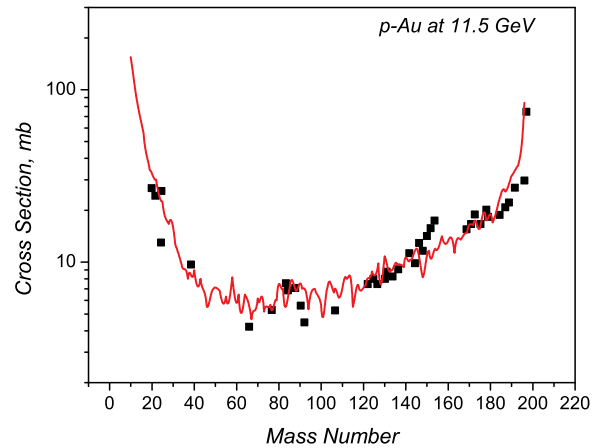


Figure 9: Mass distribution of fragments in the reaction $p + {}^{197}\text{Au}$ at 11.5 GeV. Data are taken from paper [18].

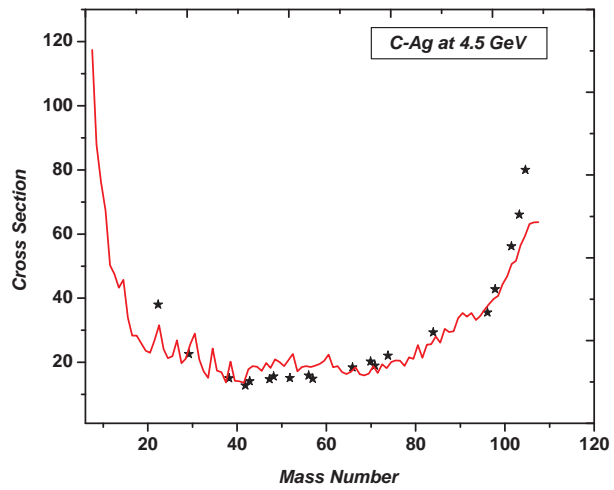


Figure 10: Mass distribution of fragments in the reaction ${}^{12}\text{C} + {}^{108}\text{Ag}$ at 4.5 GeV. Data are taken from paper [19].

6 Conclusions

New version of Modified Cascade Model for intermediate and high energy nucleus – nucleus collisions including multifragmentation channels is developed. Colliding nuclei represent face – centered cubic lattices. Multifragmentation is calculated in the frame of percolation theory with usage of site – bond percolation model. This version is able to reproduce reasonably well both spallation and multifragmentation processes.

7 Appendix: Hadronic Event Generator

Monte - Carlo simulation of inelastic events is performed in several steps. The first step in the generation of exclusive event is the evaluation of initial c.m. energy portion available for production of secondaries

$$W = \sum E_i = k\sqrt{s} \quad (20)$$

where E_i is the energy of i – th particle (excluding leading particles), k is inelasticity. Fluctuation of the inelasticity from event to event leads to the distribution $P(k)$. There are no elaborated theoretical methods for calculation of $P(k)$. It has been shown in Ref.[20] that one may fit the inelasticity distribution with beta distribution

$$P(k, s) = k^{a-1}(1-k)^{b-1}/B(a, b) \quad (21)$$

$$B(a, b) = \Gamma(a)\Gamma(b)/\Gamma(a, b) \quad (22)$$

$$\langle k(s) \rangle = a/(a + b) \quad (23)$$

where $\Gamma(a)$, $\Gamma(b)$ and $\Gamma(a, b)$ – gamma functions; s - dependence of $P(k, s)$ and $\langle k(s) \rangle$ is enclosed in parameters a and b . Up to the ISR energies one can neglect this s - dependence. On the second step the energy W is distributed between secondary particles which kinematical characteristics are generated in correspondence to a cylindrical phase space model. Parameters of cylindrical phase space model are adjusted by comparing the results of simulation of pion – nucleon and nucleon – nucleon interactions with data. The remaining part of c.m. energy $(1-k)\sqrt{s}$ is distributed between remnants

of interacting particles (so called leading particles) according to energy – momentum conservation laws

$$\overline{P}_I + \overline{P}_{II} = \sum \overline{P}_i \quad (24)$$

$$E_I + E_{II} = (1 - k)\sqrt{s} \quad (25)$$

where \overline{P}_i is a momentum of i -th produced particle, \overline{P}_I , \overline{P}_{II} and E_I , E_{II} , are momenta and energies of leading particles. Interacting nucleons (mesons) can transform into nucleons (mesons) and s – wave resonances (Δ – isobars and ρ , ω – mesons). Transition probabilities are calculated with the use of one-pion-exchange (OPE) model.

References

- [1] W. Bauer et al., Nucl. Phys. **A452** (1986) 699.
- [2] N.C. Chao and K. C. Chung, J.Phys. G: Nucl. Part. Phys. **17** (1991) 1851.
- [3] A.J. Santiago and K.C. Chung, J. Phys. G: Nucl. Part. Phys. **19** (1993) 349.
- [4] L. Pauling, Science **150** (1965) 297.
- [5] G. Anagnostatos, Can. J. Phys. **51** (1973) 998.
- [6] N.D. Cook, Atomkernenergie **28** (1976) 195; V. Dallacasa, Atomkernenergie **37** (1981) 143; V. Dallacasa and N. D. Cook, Nuovo Cim. **A97** (1987) 157; ibid **A97** (1987) 184.
- [7] G. Musulmanbekov, *Proc. 11th EMU01 Coll. Meeting*, Dubna, May 11–13, 1992 (Ed. V. Bradnova), JINR, Dubna, 1992, p.288.
- [8] S.A. Krasnov et al., Czech. Jour. Phys., **46** (1996) 531.
- [9] N.D. Cook, Comp. in Phys. Mar/Apr, 1989, p.73.
- [10] N.D. Cook, J. Phys. G: Nucl. Part. Phys. **23** (1997) 1109.

- [11] V.S. Barashenkov and V.D. Toneev, *Interactions of high energy particles and nuclei with atomic nuclei*, Moscow, Atomizdat, 1972 (in russian).
- [12] X. Campi and J. Desbois, *Proc. 23th Int. winter Meeting on Nucl. Phys.*, Bormio, 1985, p.707.
- [13] S. B. Kaufman et al., *Phys. Rev.*, **C22** (1980) 1897.
- [14] F. Rejmund et al., *Nucl. Phys.* **A683** (2001) 540; J. Benlliure et al., *Nucl. Phys.* **A683** (2001) 513.
- [15] W. Wlazlo et al., *Phys. Rev. Lett.* **84** (2000) 5736; T. Enqvist et al., *Nucl. Phys.*, **A686** (2001) 481.
- [16] J. Taïeb, PhD thesis, IPN Orsay, France, 2000.
- [17] G. English, N.T. Porile and E.P. Steinberg , *Phys. Rev.* **C10** (1974) 2268.
- [18] S.B. Kaufman et al., *Phys. Rev.* **C14** (1976) 1121.
- [19] P. Kozma et al., JINR-E2-94-380.
- [20] G.N. Fowler, R.M. Weiner and G. Wilk, *Phys. Rev. Lett.* **55** (1985) 173.